

What Definitively Controls the Photochemical Activity of Methylbenzonitriles and Methylanisoles? Insights from Theory

Xuefei Xu, Zexing Cao,* and Qianer Zhang

Department of Chemistry, State Key Laboratory of Physical Chemistry of Solid Surfaces, and Center for Theoretical Chemistry, Xiamen University, Xiamen 361005, China

Received: March 12, 2007; In Final Form: May 8, 2007

CASPT2/CASSCF and B3LYP methodologies have been used to study the excited-state properties and photochemical isomerizations of p-, m-, and o-methylbenzonitriles and methylanisoles. Calculations show that the biradical mechanism is the most favored channel for the photoinduced interconversion of p-, m- and o-methylbenzonitriles, both dynamically and thermodynamically. The formation of biradical as a key intermediate is highly selective, and only the biradicals with a turned-up cyano-substituted carbon are involved in photoisomerization. Methylanisole isomers are inactive relative to methylbenzonitriles at 254 nm. Such remarkable activity difference between methylbenzonitrile and methylanisole in photochemistry arises from the accessibility of the S_1/S_0 conical intersection as well as the stability of prefulvene biradicals. For methylanisoles, the S_1/S_0 precursor and the reactive biradicals are inaccessible at 254 nm, which should be the origin of inactivity. The results suggest that the conical intersection accessibility plays a crucial role in the photochemistry of substituted benzenes at 254 nm.

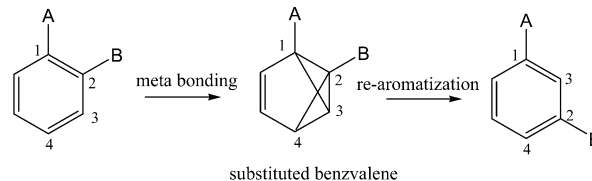
Introduction

Photochemistry of benzene and its derivatives as most stable aromatic species has received considerable attention, both theoretically and experimentally. In 1964, Wilzbach and Kaplan¹ first observed that dialkylbenzene isomers undergo interconversion under ultraviolet irradiation. Such photoinduced isomerization was initially ascribed into alkyl group translocation around the ring, but subsequent isotope-labeling experiment² of photolysis of 1,3,5-trimethylbenzene demonstrates that the alkyl migration was actually a result of ring carbon interchange. A tricyclohexane (benzvalene) structure with two meta bondings was assumed as a plausible intermediate in the carbon atom transposition (Scheme 1). The substituted benzvalene may evolve to other isomers of substituted benzene by breaking two carbon–carbon bonds.

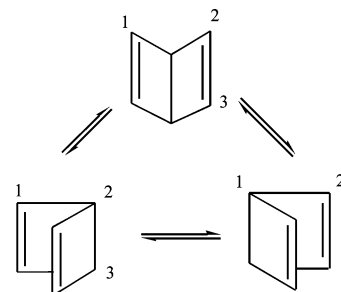
However, the benzvalene mechanism is unable to interpret well the 1,3-shift of ring carbon atom observed in the photolysis of dimethyl- and dimethylethylbenzenes in solution,^{1,2} and this process may be accessible only through two- or three-photon pathway in the single benzvalene mechanism. An alternative mechanism involving labile Dewar structures (see Scheme 2) as intermediates can adequately account for 1,3-shift outcomes.^{2,3} Therefore, Wilzbach et al.² assumed that both mechanisms were concurrently responsible for the carbon atom phototransposition processes at different conditions.

An MC-SCF study^{4a} of photoreaction of benzene on the S_1 and S_2 potential energy surfaces (PES) suggested that the formation of benzvalene experiences a transition state with a barrier of ~ 23 kcal mol⁻¹ for the rate-determining step on the S_1 PES. For the re-aromatization process from benzvalene to benzene, the activation energy was found experimentally to be 26.7 kcal mol⁻¹.⁵ Similarly, the conversion from Dewar benzene back to benzene also requires an energy of 23.9 kcal mol⁻¹.^{4a}

SCHEME 1



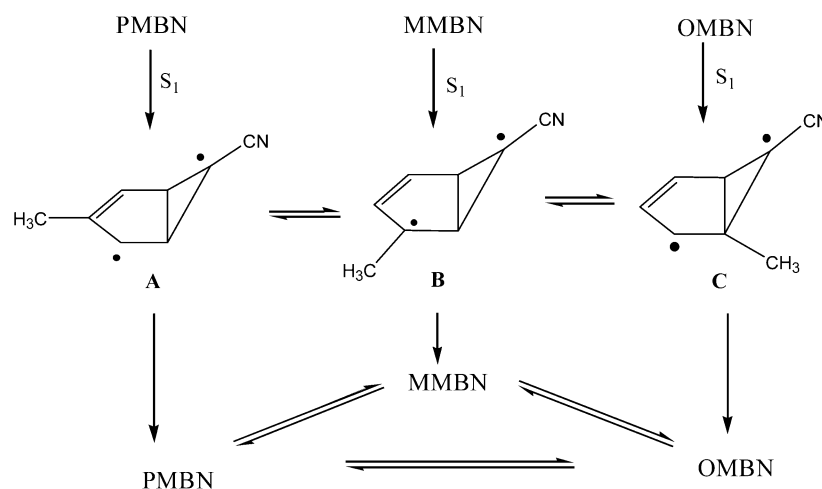
SCHEME 2



In 1998, MacLeod et al.⁶ explored photochemical isomerization of p-, m-, and o-methylbenzonitriles (PMBN, MMBN, OMBN) in acetonitrile. They found that irradiation of any one of three isomers can produce other two species in the primary photochemical event. These photoisomerization processes occur on the singlet excited-state PES, and relative conversion efficiencies are isomer-dependent, with a ratio of 32:4:1 for PMBN, MMBN, and OMBN, respectively. Ulterior deuterium labeling experiment reveals that the transposition is highly selective and only migration of the cyano-substituted carbon was involved in the photoinduced process. A possible mechanism with both 1,2- and 1,3-shifts has been suggested for these phototransposition processes (Scheme 3).⁶ In this mechanism, three interconvertible singlet prefulvene biradicals (A, B, and C) arising from the excitation to the S_1 state serve as important intermediates. The different interchange reactivities of these

* Corresponding author. E-mail: zxcao@xmu.edu.cn.

SCHEME 3



isomers were probably resulted from isomer-dependent activation barriers for formation of corresponding singlet prefulvene biradicals on the reactive S_1 PES.⁶ Photochemical addition experiment of 2,2,2-trifluoroethanol to *p*-, *m*-, *o*-methylbenzonitriles lends support to this mechanism.⁷

Previous theoretical study has confirmed that the prefulvene biradical intermediates via conical intersections are involved in the photochemical paths and decay channels of excited benzene.⁴ Especially, the conical intersection region was claimed to be related to the “channel three” decay mechanism of benzene (fluorescence loss with a vibrational excess threshold of $\sim 3000\text{ cm}^{-1}$).^{4a} Predicted rate constants of nonradiative decay of the S_1 state support that an intermediate electronic configuration S_x admixed with both S_1 and S_0 was involved in the mysterious decay route.^{4c}

However, recent systematic investigations⁸ on photoequilibrium of the *ortho*-, *meta*-, and *para*-isomers of substituted benzenes indicate that methylanisole isomers are unreactive relative to methylbenzonitriles. What prevents methylanisoles from undergoing interconversion? What is the mechanism for methylbenzonitrile photoisomerization? What dominates photochemical interconversions of *p*-, *m*-, and *o*-substituted benzenes? These questions remain open due to the lack of knowledge in electronic structure and PES feature of the excited state.

Here, we performed an extensively theoretical study on both methylbenzonitrile and methylanisole. Structures and relative energies of key states have been investigated by the density functional theory and *ab initio* methodologies. Plausible photoisomerization channels and photochemical activities for both species on the singlet potential surfaces have been discussed.

Computational Details

Geometry optimizations and vibrational analyses for stationary points on the ground-state potential energy surfaces have been performed by density functional theory (DFT) approach. The Becke's three-parameter hybrid exchange functional⁹ and the Lee–Yang–Parr correlation functional¹⁰ (B3LYP) implemented in the GAUSSIAN 03 package¹¹ have been used in the DFT calculation. For the singlet biradical structures, the Hartree–Fock exchange potential from the unrestricted wavefunction was considered in the unrestricted B3LYP treatment. For comparison, these stationary points also have been optimized by the CASSCF¹² method. In this case, 10 valence electrons are allowed to distribute in all possible ways into eight low-energy

π orbitals, denoted as CAS(10,8). At the same CASSCF level, the first excited states (S_1) have been optimized.

To reduce computational costs, the substituted benzvalene, carbene, conical crossing, and transition-state structures on the ground-state PES have been optimized at the CAS(8,7) level. Test calculations indicate that use of relatively small active space was still adequate for geometry optimization. No symmetry constraints have been introduced in all geometry optimizations. In order to validate estimation of relative energies, CASPT2¹³ calculations were carried out on the basis of the CAS(10,10) wave function at the CASSCF-optimized geometries. The absorption and fluorescence spectra were computed by the CASPT2 approach in combination of the state-averaged CAS-(10,10) calculations at the CAS(10,8)- optimized geometries. The time-dependent density functional approach with the B3LYP functional (TD-B3LYP)¹⁴ and the CCSD-EOM¹⁵ approach also have been used to determine the vertical transition energies. MOLPRO 2002¹⁶ and GAUSSIAN 03 program packages, as well as the 6-31G(d)¹⁷ basis set, were used for all CASSCF, CASPT2, and CCSD-EOM calculations.

Results and Discussion

1. Methylbenzonitriles. *1.1. Absorption Spectra.* *Para*-, *meta*-, and *ortho* isomers of methylbenzonitriles (PMBN (**1**), MMBN (**2**), and OMBN (**3**)) on the ground-state potential energy surface have been optimized by both B3LYP and CASSCF methods. Figures 1 and 2 display the B3LYP-optimized and the CASSCF-optimized structures, respectively. Calculations indicate that three isomers of methylbenzonitrile are nearly isoenergetic and the energy difference varies within 0.4 kcal mol^{-1} by B3LYP and 1.6 kcal mol^{-1} by CASPT2. Employing the optimized ground-state geometry, the absorption spectra of PMBN in the gas phase have been predicted by TD-B3LYP, CCSD, CASSCF, and CASPT2 approaches with the 6-31G(d) basis set. Predicted vertical excitation energies and corresponding oscillator strengths are given in Table 1.

The first excited state (S_1) of PMBN is mainly described by the combination of two configurations arising from HOMO-1→LUMO and HOMO→LUMO+1 electronic excitations. As Table 1 shows, the CASSCF and CASPT2 calculations predict quite similar vertical transition energies of 4.77 eV (260 nm) and 4.79 eV (259 nm), respectively. They are in reasonable agreement with the experimental absorption maximum value (268 nm) in acetonitrile. TD-B3LYP and CCSD-EOM calculations overestimate the vertical excitation energy of S_1 slightly.

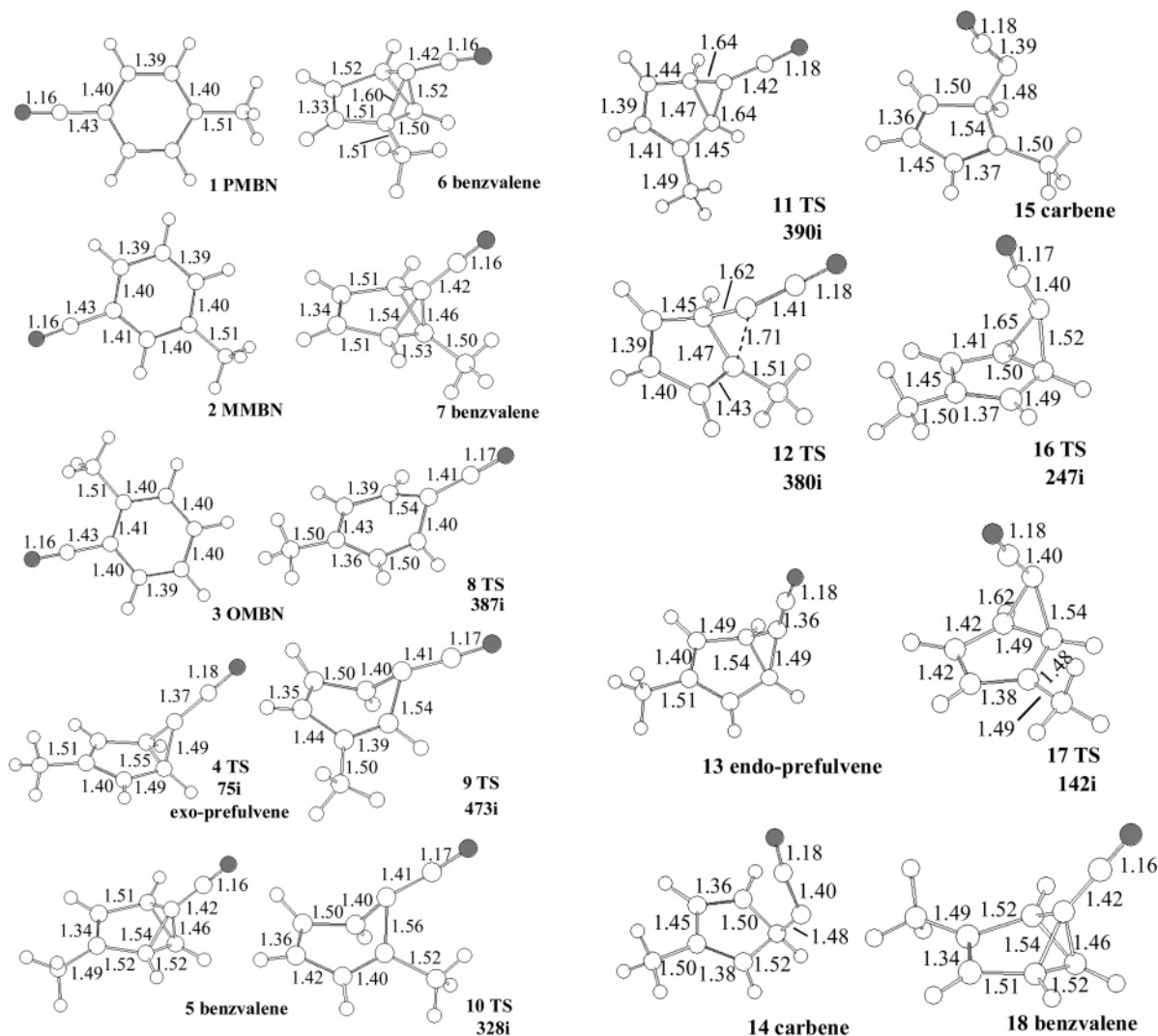


Figure 1. Selected B3LYP-optimized structures of methylbenzonitrile derivatives.

The second excited state (S_2) of PMBN with a dipole increment of 2.42D compared to the ground state has an ionic character, just as in the cases of benzene 1^1B_{1u} state and benzonitrile 2^1A_1 state.¹⁸ The effect of dynamic electron correlation on the S_2 state is significant, and the CASSCF calculation seriously overestimates this excited state. The CASSCF excitation energy of S_2 is remarkable higher than the CASPT2 value by 0.8 eV. As the Table 1 displays, the CCSD-EOM vertical transition energy of S_2 is comparable to that of CASPT2. On the contrary, the TD-B3LYP calculation predicts that the vertical S_2 state lies at 5.50 eV (225 nm) above the ground state in the gas phase, much lower than those by CASPT2 and CCSD-EOM. This can be ascribed to the charge-transfer and double excitation characters of the S_2 state. It was well-known that TD-DFT is not adequate for description of charge-transfer excited states and doubly excited states.¹⁹

In order to obtain a more accurate description of the S_2 state with ionic character, the 6-31G(d) basis set augmented with a diffuse function (the 6-31+G(d)) also has been considered in determination of excitation energy by CASPT2. The results indicate that the involvement of diffuse function reduces the vertical transition energy of S_2 to 6.33 eV. In consideration of the computational deviation and the significant overlap effect for the excited-state with an ionic character (the 2^1A_1 state of benzonitrile may be stabilized by 0.77 eV in the polar solvent of acetonitrile¹⁸), present CASPT2/6-31+G(d) result of S_2 in

the gas phase is reasonable in comparison with the observed value of 232 nm (5.34 eV) in acetonitrile.⁶

All calculations at different theoretical levels indicate that the strongest absorption arises from the electronic excitation to the S_2 state in the gas phase. Experimentally, two relatively strong absorptions of methylbenzonitrile in acetonitrile appear in the range of long wavelength.⁶ However, only the S_1 state is accessible energetically under the irradiation light of 254 nm (4.88 eV/112.5 kcal mol⁻¹), based on these observed spectra.⁶ The S_1 state is expected to be directly involved in the photochemical equilibration of *p*-, *m*-, and *o*-isomers for methylbenzonitrile at 254 nm.

1.2. Emission Spectra. The S_1 states of methylbenzonitrile isomers have been optimized by CASSCF. Like their ground states, these S_1 states are quite close in energy, and the energy difference among isomers is less than 0.8 kcal mol⁻¹ at the CASPT2 level. As Figure 2 shows, the S_1 state geometry (**19**) of PMBN has an expanding phenyl ring as compared with its ground state (**1**). On the basis of the optimized S_1 geometry, the predicted fluorescence emission occurs at 4.37 eV (100.8 kcal mol⁻¹) for PMBN by CASPT2. The calculated adiabatic transition energy of S_1 state is 4.46 eV (102.9 kcal mol⁻¹), which agrees with the experimental 0,0 transition (101 kcal mol⁻¹) very well.⁶

1.3. Photochemical Interconversions of *p*-, *m*-, and *o*-Methylbenzonitriles. A. The Biradical Mechanism. First, we

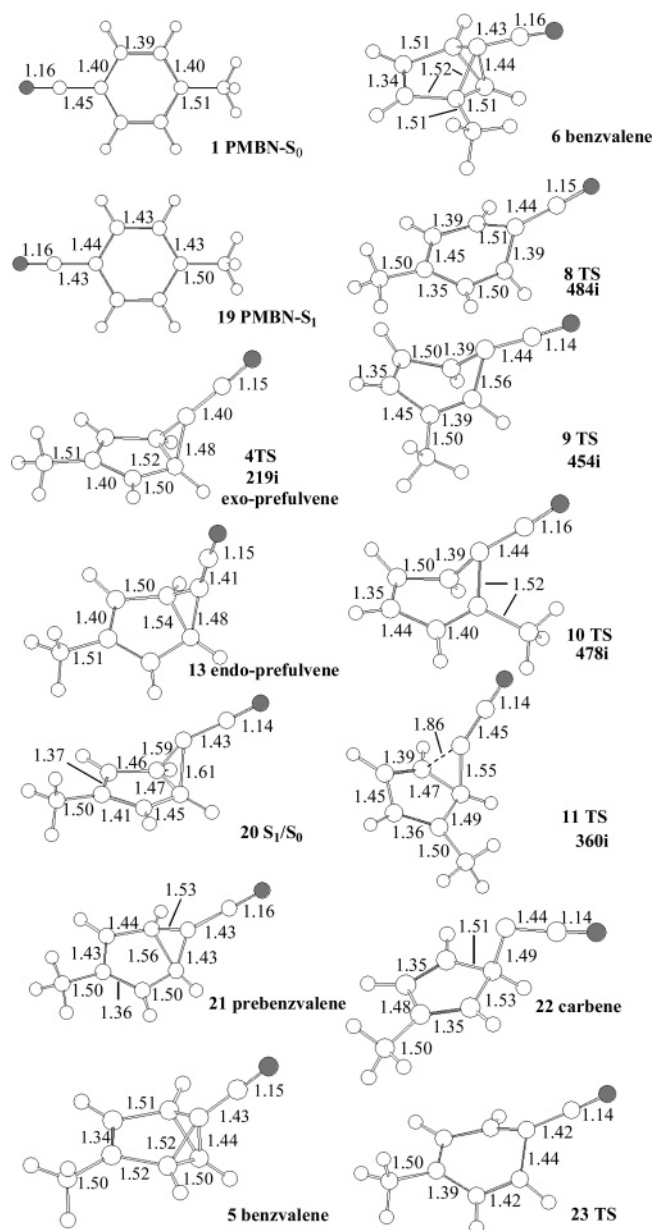


Figure 2. Selected CASSCF-optimized structures of methylbenzoinitrile derivatives (23TS is the transition state to the S_1/S_0 conical intersection of methylbenzoinitrile in S_1 by the CIS approach).

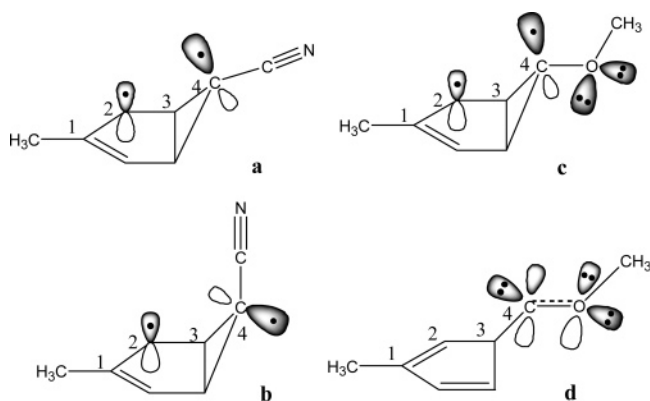
TABLE 1: Vertical Transition Energies (ΔE in eV) and Oscillator Strengths (f) of Low-lying Excited States of PMBN (1) and p-Methylanisole (A1) in the Gas Phase

	TDB3LYP		CCSD		CAS	CASPT2	exp. ^a
	ΔE	f	ΔE	ΔE	ΔE^b	f	
1- S_1	5.11	0.0021	5.09	4.77	4.79 (4.78)	0.0009	4.63
1- S_2^c	5.50	0.3137	6.35	4.77	6.67 (6.33)	0.0670	5.34
A1- S_1	5.07	0.0302		4.93	4.70 (4.67)		
A1- S_2^c	5.87	0.1655		7.79	6.30 (5.93)		

^a Absorption maximum in acetonitrile from ref 6. ^b The values in parenthesis are obtained at the CASPT2/6-31+G(d) level. ^c The CASSCF wave function of the S_2 state includes partial double excitation configurations, and it exhibits a large dipole increment (increase of 50–100%) relative to the ground state, showing the character of charge transfer.

considered the possibility of the prefulvene biradical mechanism for the photoinduced interconversion. Such a route has been suggested for photoisomerization of methylbenzoinitriles experimentally.⁶

SCHEME 4



Using an unrestricted B3LYP treatment, we located two substituted prefulvene structures of PMBN, an *exo* form (4) and an *endo* form (13), as shown in Figure 1. The energy difference for both species is less 0.1 kcal mol⁻¹. Despite lack of any geometrical restriction in calculation, the optimized geometries of both biradicals show basically C_s symmetry. Frequency calculations indicate that the *exo* form is a first-order saddle point with an imaginary frequency of 75 cm⁻¹, whereas the *endo* form is a minimum, which is in agreement with previous calculations on prefulvene structures of benzene at the UB3LYP/DZP level.²⁰ Similarly, our CASSCF calculations predict that the *exo*-prefulvene structure (4) is a transition-state structure with an imaginary frequency of 219 cm⁻¹ and the *endo* form (13) is a minimum on the singlet PES. The imaginary mode indicates the transition-state structure (4) will evolve into a benzvalene conformation of PMBN. The CASSCF-optimized geometries are given in Figure 2. In previous CASSCF investigations,^{21,22} the *exo* form of prefulvene has been characterized as a minimum, while MCSCF calculations by Palmer^{4a} and Dreyer²³ are consistent with present results.

The instability of *exo* form can be understood through visual bonding analysis as shown in Scheme 4. In the *exo* biradical (Scheme 4a), although the unpaired electron at C4 can be stabilized by the CN group through conjugated interactions, to some extent, the unpaired electron at C2 has tendency to couple with the single electron at C4, which makes the biradical (4) serve as a transition state to benzvalene.

In the vicinity of the *exo*-prefulvene structure of PMBN, a minimum (21 in Figure 2) on the PES has been located by the CASSCF calculation, which is analogous with the prebenzvalene structure of benzene reported by Palmer.^{4a} The prefulvene structure returns to benzene or distorted benzvalene through two transition states with negligible barrier of ~ 1 kcal mol⁻¹, where the prebenzvalene structure serves as an intermediate.^{4a}

In a subsequent search for conical intersection of S_1 with S_0 in PMBN, a prefulvene-like S_1/S_0 structure (20 in Figure 2) was found by CASSCF, where the ring carbon atom connecting with the CN group was turned up. Such out-of-plane distortion conformation can accelerate the coupling of S_1 with S_0 . The optimized S_1/S_0 structure was ~ 9 kcal mol⁻¹ above the two prefulvene structures (4 and 13) in energy by CASPT2. Thus, the prefulvene-like S_1/S_0 conical intersection (20) can easily transform to the prefulvene structures. A transition-state structure (23TS in Figure 2) connecting the S_1 minimum to the S_1/S_0 conical intersection (20) has been located by the CIS approach, which is 5.9 kcal mol⁻¹ above the Franck–Condon (FC) structure of S_1 at the CASPT2 level. The predicted gas-phase barrier from the S_1 FC structure to the S_1/S_0 conical intersection agrees well with the experimentally estimated activation energy

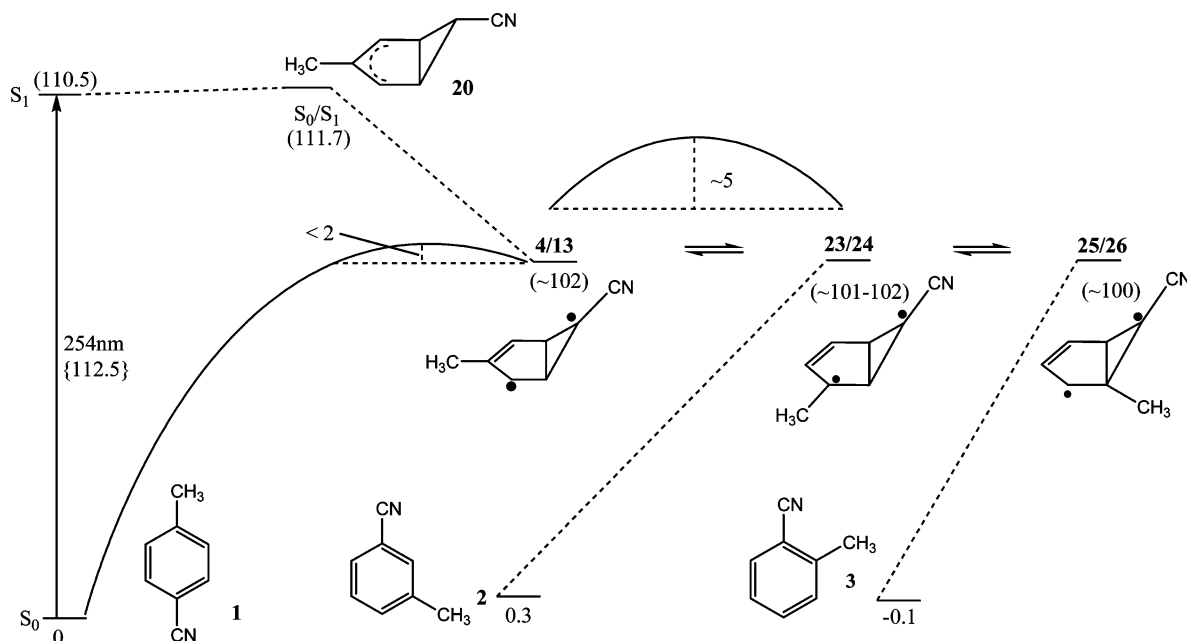


Figure 3. The CASPT2 relative energies (kcal mol⁻¹) for photoisomerization of methylbenzonitrile **1** with **2** and **3** in the gas phase through prefulvene biradicals. The values without parentheses are obtained by B3LYP.

of ~ 6.4 kcal mol⁻¹ on the S₁ PES by variable temperature fluorescence study of PMBN in acetonitrile.^{8b}

For MMBN and OMBN, two forms of prefulvene biradical (**23/24** and **25/26** in Figure 3) and prefulvene-like S₁/S₀ conical intersection structures also have been obtained. These structures (**23/24** and **25/26**) are very similar to corresponding those of PMBN both in geometry and in energy. The PES scan at the UB3LYP level shows that the interconversion of the substituted prefulvenes by migration of the cyano-linking carbon experiences a small barrier of ~ 5 kcal mol⁻¹. Finally, these substituted prefulvenes return to corresponding substituted methylbenzonitriles, requiring energy of less than 2 kcal mol⁻¹.

Figure 3 displays the calculated relative energetics of photoisomerization from PMBN to MMBN and OMBN in the gas phase through substituted prefulvene biradicals following the S₁/S₀ conical intersection under the irradiation light of 254 nm. As Figure 3 shows, our calculations support the biradical route as an effective photochemical channel for interconversion of *p*-, *m*-, and *o*-methylbenzonitriles. Once any one of three methylbenzonitrile isomers is excited to the S₁ state at 254 nm, the corresponding biradical structures formed through its S₁/S₀ conical intersection can evolve into other two substituted biradicals. These biradicals will be in equilibrium due to facile interconversion. Followed by rearomatization, they may return to corresponding substituted benzene forms.

B. The Benzvalene Mechanism. The benzvalene structures (**5**, **6**, and **7**) of methylbenzonitriles have been optimized by B3LYP and CASSCF. The corresponding structural parameters are shown in Figures 1 and 2.

Since the formation of substituted benzvalenes from the substituted prefulvene following the S₁/S₀ conical intersection almost is a barrier-free process, they might be important intermediates in the photoisomerization reactions of methylbenzonitriles. However, the re-aromatization back to the substituted benzene and direct interconversion of different substituted benzvalenes both have to overcome a large energy barrier. The CASPT2 calculated activation energies for the ring opening of substituted benzvalenes are ~ 28 kcal mol⁻¹, which is comparable with the experimental value of 26.7 kcal mol⁻¹ for benzvalene.⁵ Our CASPT2 calculations indicate that a larger

energy (~ 40 kcal mol⁻¹) is required in the direct isomerizations of substituted benzvalenes. For example, the **5** → **6** conversion via a transition state (**11TS**) has a barrier of 38.1 kcal mol⁻¹, and the barrier of **6** → **7** via **12TS** is 40.7 kcal mol⁻¹. Hence, no direct pathway to produce 1,3-shift product in the singlet benzvalene mechanism.

Since both 1,2- and 1,3-shift biradicals can be formed in a primary photochemical event as mentioned above and further they may evolve to benzvalenes almost without energy requirement, all of the benzvalene isomers could be populated via the biradical mechanism in the one-photon process. Thus, the interconversion of methylbenzonitriles can occur through the benzvalene photochemical path with involvement of biradicals. Figure 4 shows the relative energetics of photoisomerization process from PMBN to MMBN and OMBN in the benzvalene mechanism with the participation of biradicals. Because rearomatization of substituted benzvalenes requires relatively high activation energy, the benzvalene-biradical route is not competitive with the low-barrier direct biradical mechanisms as shown in Figure 3.

C. The 1,2-Carbon Shift Mechanism. In search for a prefulvene biradical structure of PMBN by CASSCF, a carbene structure (**22** in Figure 2) was also located accidentally. The 1,3-cyclopentadienylcarbene (Scheme 5a) has been identified as a key intermediate in the photochemical isomerization of benzene to fulvene,²⁴ and it also has been included in the investigation of 1,2-carbon shift mechanism for the topomerization of benzene (Scheme 5).²⁰

Similar to the prefulvene biradical, the substituted carbene, which is accessible following the S₁/S₀ conical intersection, has two conformations (**22** in Figure 2 and **14** in Figure 1) with different orientation of the cyano group. The B3LYP method cannot locate the "outward" form **22**, which is unfavorable energetically due to electron–electron repulsion between the π electrons of diene and the σ^2 lone pair of carbene.²⁰ In an attempt to optimize the transition state connecting the carbenes (**22** and **14**) to the substituted benzenes, the labile carbene structures converge at the transition-state structures **8TS** and **9TS**, respectively, and they are responsible for benzvalene → benzene isomerizations. This implies that these carbenes prefer benz-

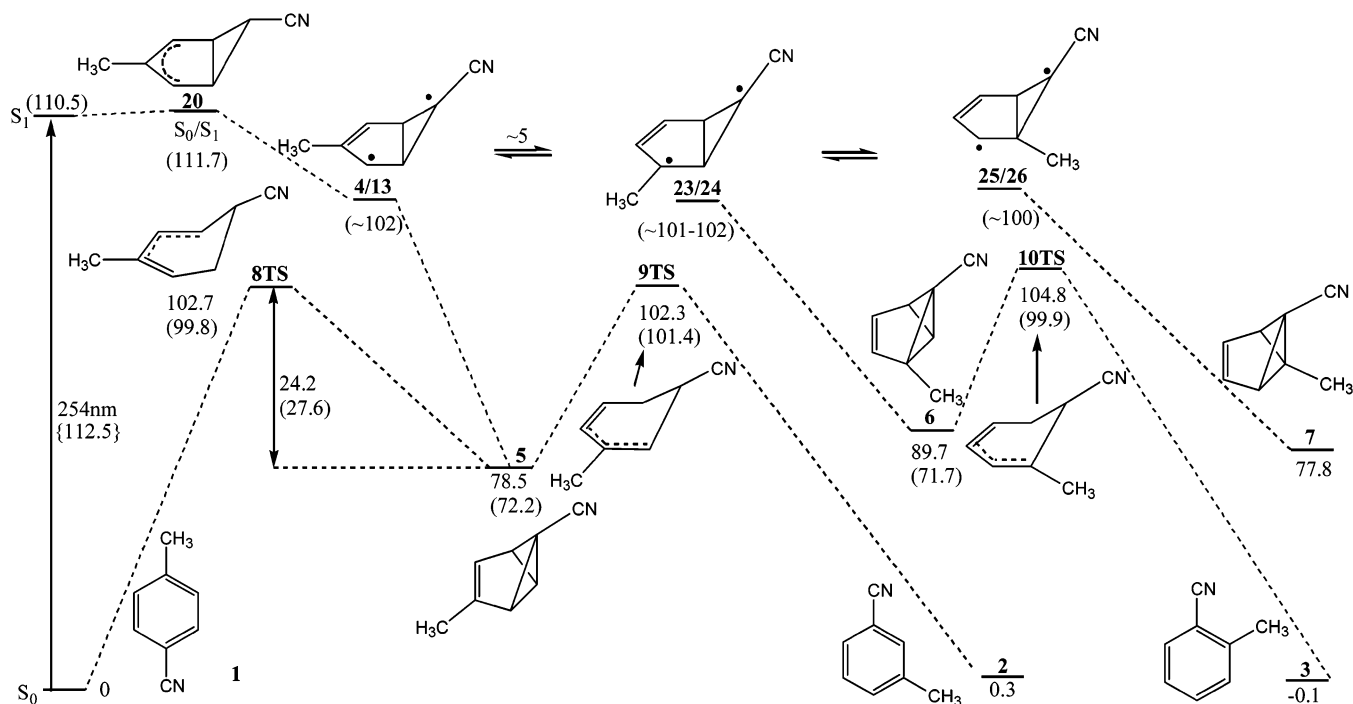
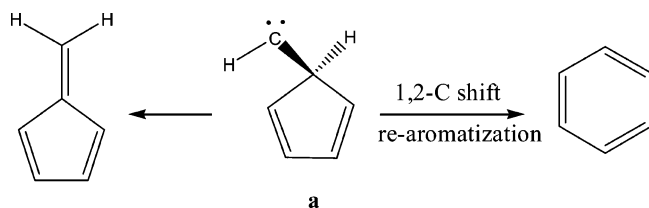


Figure 4. The B3LYP relative energetics (kcal mol^{-1}) of photoinduced conversion from PMBN to MMBN and OMBN via the benzvalene mechanism coupled with prefulvene biradicals. The values in parentheses are obtained at the CASPT2 level.

SCHEME 5



valene to benzene in structural evolution. Therefore, the 1,2-C shift mechanism should be less relevant to the photoisomerization of methylbenzonitriles.

We also investigated the probability of 1,2-hydrogen shift mechanism by B3LYP and TD-B3LYP methods. Calculations show that for the photochemical interconversion of methylbenzonitriles, the 1,2-H shift path is less favored as a result of the relatively high barrier. The detailed discussion refers to the Supporting Information.

2. Methylanisoles. *2.1. Electronic Spectra.* The ground-state structures of *p*-, *m*-, and *o*-methylanisoles (**A1**, **A2/A3**, **A4**) have been optimized by B3LYP. The optimized geometries see Supporting Information. All these isomers are quite close in energy, like methylbenzonitriles. On the basis of the optimized geometry, the absorption spectra of *p*-methylanisole (**A1**) in the gas phase have been determined by TD-B3LYP. Considering multireference electronic feature of an ionic state and double excitation for the second excited state (S_2), the absorption spectra of **A1** were also calculated by CASPT2/6-31+G(d) at the CASSCF-optimized geometry of the ground state. Table 1 gives the predicted vertical excitation energies for *p*-methylanisole.

As Table 1 shows, *p*-methylanisole has similar gas-phase absorption spectra with PMBN: the vertical S_1 and S_2 states have a large energy gap; the vertical transition energy for the first excited state (S_1) is 4.70 eV (5.08 eV at the TD-B3LYP level). The S_1 state mainly comprises two excitation configurations, and it is the only accessible excited-state at 254 nm, although it has relatively small oscillator strength. In the following investigation for photoisomerization of methylani-

soles, only the potential energy surfaces of S_1 and the ground state have been considered here.

The equilibrium geometry (**A5** in Figure 5) of S_1 for *p*-methylanisole has been located by CASSCF. Using the optimized geometry of S_1 , the fluorescence emission of *p*-methylanisole in the gas phase is estimated to be 4.35 eV at the CASPT2 level. The calculated adiabatic transition energy of S_1 state for *p*-methylanisole is 4.47 eV, which is comparable with the rotationally resolved $S_0 \rightarrow S_1$ fluorescence excitation spectrum of band $0a_1^{25}$ of *m*-methylanisole (4.47 eV for *cis* form and 4.48 eV for *trans* form) in the gas phase.

2.2. Isomerization of p-, m- and o-Methylanisoles. Selected optimized structures, probably involved in the photochemical isomerization process of methylanisoles, have been depicted in Figure 5. For *p*-methylanisole, the S_1/S_0 conical intersection (**A6**) has the prefulvene-like structure like PMBN. However, no prefulvene biradical structure has been located. All attempts to search for a biradical structure failed and the geometry optimization was converged at a carbene structure (**A11**) or a substituted prebenzvalene (**A7**), implying that the biradical structure is unlikely to be formed and to be involved in photoisomerization of methylanisoles. This can be understood through the visual bonding interaction as indicated in Scheme 4. Suppose that there is a biradical structure of methylanisole as shown in Scheme 4c, due to lack of the conjugated interaction between C4 and $-\text{OCH}_3$, this biradical form is less stable relative to the biradical of PMBN (Scheme 4a). In addition, the lone pair electrons of oxygen in $-\text{OCH}_3$ will push the single electron at C4 to couple with the single electron at C2, leading to a prebenzvalene structure (**A7**). The prebenzvalene structure can easily distort toward benzvalene. Hence the biradicals cannot be served as reactive intermediates for interconversion of methylanisoles.

Alternatively, the C4–C5 bond cleavage gives rise to a more stable carbene (**A11** in Figure 5 or **d** in Scheme 4), where the C4 atom can offer an empty orbital to share the lone pair of oxygen through conjugated interaction. The carbene structure of *p*-methylanisole is more stable as compared with that of

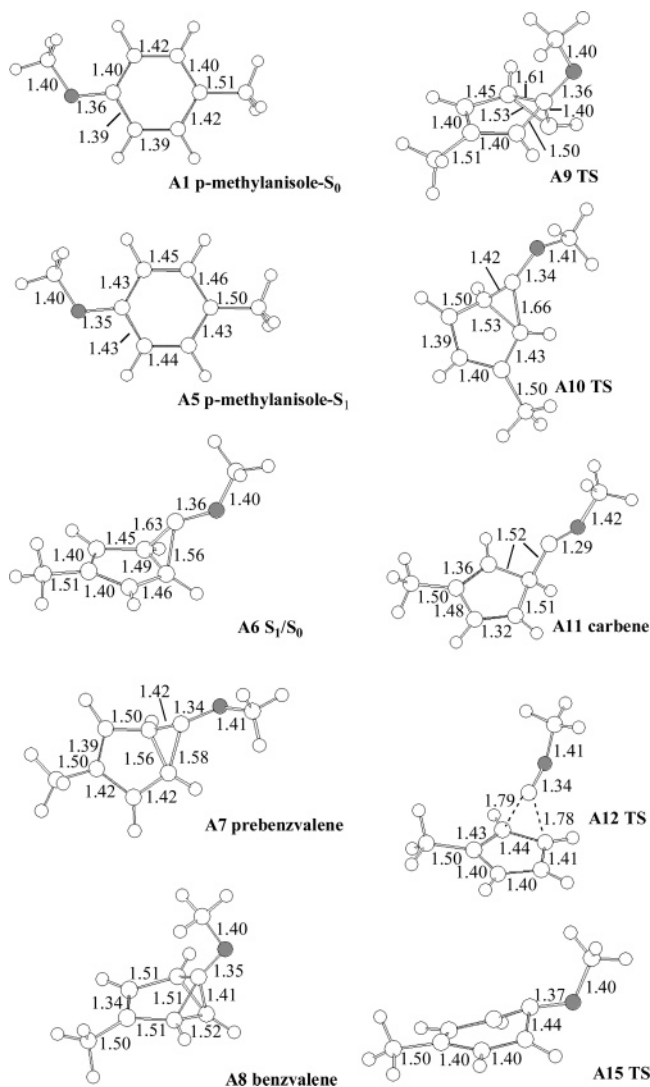


Figure 5. Selected CASSCF-optimized structures for isomerization of methylanisoles (**A15TS** is the transition state to the S_1/S_0 conical intersection of methylanisole in S_1 by the CIS approach).

PMBN. A transition-state structure (**A10TS**) connecting the carbene (**A11**) with benzvalene (**A8**) has been located. The calculated barriers are $4.1 \text{ kcal mol}^{-1}$ from **A11** to **A8** and $17.1 \text{ kcal mol}^{-1}$ from **A8** to **A11** at the CASPT2 level. Our calculations show that the interconversion barrier of carbenes is $6.9 \text{ kcal mol}^{-1}$ from **A11** to **A13**, lower than that of benzvalenes. The **A11** may return to **A2** via **A14TS** with a barrier of $7.8 \text{ kcal mol}^{-1}$. The reaction pathways and relative energies for isomerization of p-methylanisole with m-methylanisole and o-methylanisole after S_1/S_0 have been displayed in Figure 6.

The substituted benzvalene (**A8**) and carbene (**A11**) structures can be populated from S_1/S_0 conical intersection (**A6**), and the former (**A8**) should be the primary product owing to its relatively high stability. Nevertheless, both re-aromatization of benzvalene to methylanisole and interconversion of benzvalene isomers have to experience large barriers, therefore the carbenes (**A11** and **A13**) should play an important role in the conversion of p-methylanisole into m- and o-methylanisoles.

On the basis of present results, we can conclude that if the S_1/S_0 intersection is accessible, photochemical isomerization of methylanisoles might occur through the mechanism involving carbenes as important intermediates, even though this process is less efficient as compared with the biradical channel in

methylbenzonitrile. Experimentally, the photochemical interconversion of methylanisoles has not been observed at 254 nm. This implies that the accessibility of the S_1/S_0 conical intersection is crucial for the photoisomerization of methylanisoles. More recently, the importance of conical intersection has been investigated in heterocyclic photochemical bond scission.²⁶

The transition-state (TS) structure (**A15TS** in Figure 5) from S_1 minimum to S_1/S_0 conical intersection of p-methylanisole has been optimized at the CIS level, since the CASSCF optimization suffered convergent failure. Based on the CIS-optimized TS structure, the barrier for formation of the S_1/S_0 conical intersection (**A6**) from the S_1 FC structure (**A1**) has been estimated to be $10.7 \text{ kcal mol}^{-1}$ at the CASPT2 level, which is higher than that of PMBN by $\sim 5 \text{ kcal mol}^{-1}$ as shown in Scheme 6. Therefore, the S_1/S_0 conical intersection of methylanisole is less accessible, and such inaccessibility should be responsible for the photochemical inactivity of methylanisoles at 254 nm. The variable temperature fluorescence studies also have shown evidence of higher activation energy on the S_1 PES for methylanisoles relative to methylbenzonitrile.^{8b}

3. The Selectivity of the Transposition of Ring Carbon.

Present calculations support that the biradical mechanism is the most favored channel, both dynamically and thermodynamically, for the transposition of ring carbon in the photochemical isomerization process of p-, m-, and o-methylbenzonitriles. Is the formation of biradical intermediate selective? What's the dominating factor? In the present calculation, only few biradical structures (**4/13**, **23/24**, **25/26**) have relatively high stabilities, where the single electron residing at the turnup carbon (C4) can be stabilized by a cyano group. In addition, an endo form with the turnup carbon linking a hydrogen atom (**c** in Scheme 7) also has been located. On the contrary, methyl and $-\text{OCH}_3$ groups cannot stabilize the radical center of adjacent carbon, and thus the prefulvene biradicals with a turned up C4 linking methyl or $-\text{OCH}_3$ group (**a** and **b** in Scheme 7) are not stable enough to survive. Although the endo biradical structure (**c** in Scheme 7) is stable enough, only 1,2-shift product can be obtained for bi-substituted benzene through the migration of carbon without substituted group in the biradical mechanism. The biradical **c** in Scheme 7 is slightly higher in energy than the biradical structures (**4/13**, **23/24**, **25/26**). Such stability difference among the biradicals will play an important role in the ring carbon interchange through the biradical mechanism. Consequently, the transposition of ring carbon is highly selective in photochemical isomerization of p-, m-, and o-substituted benzenes, which agree with previous experimental observations.⁶

Conclusions

The mechanistic details for phototransposition of p-, m-, and o-methylbenzonitriles on the singlet potential energy surfaces have been explored theoretically. The results show that the reaction channel involving prefulvene biradicals as important intermediates is the most favored photoisomerization process energetically. Benzvalene intermediates coupled with prefulvene biradicals might be involved in photoisomerization, but such process is less competitive in comparison with the prefulvene biradical mechanism, due to the large barrier in re-aromatization of substituted benzvalenes. In the biradical route, only the biradicals with the cyano-substituted or nonsubstituted turned up carbon exist, which makes the ring carbon migration in methylbenzonitriles highly selective.

For methylanisoles, the photochemical isomerization of p-, m-, and o-isomers cannot take place at 254 nm, due to large kinetic barrier separating the FC S_1 structure from the corre-

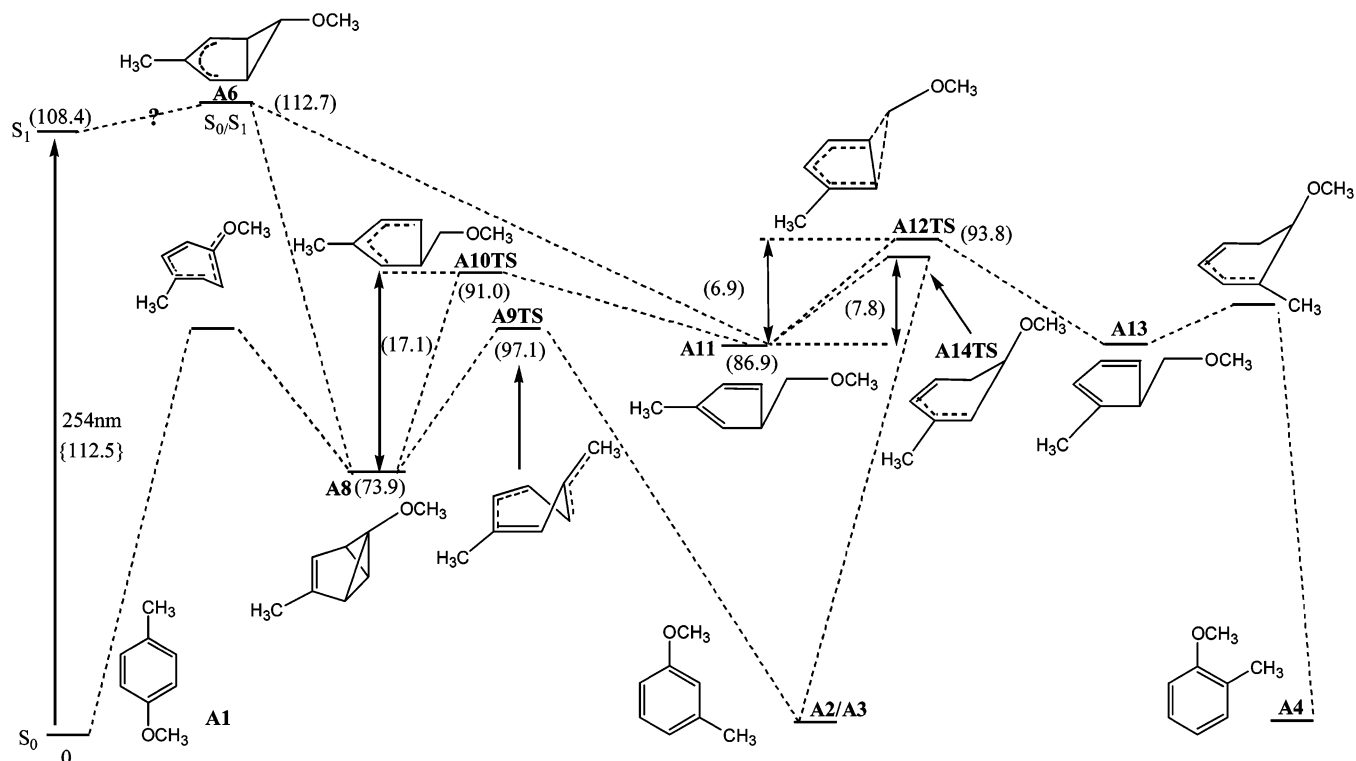
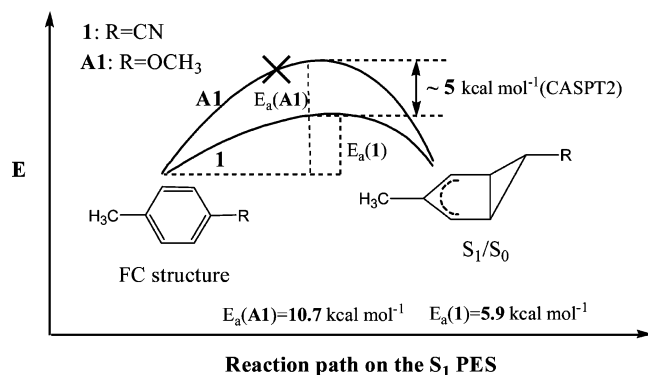
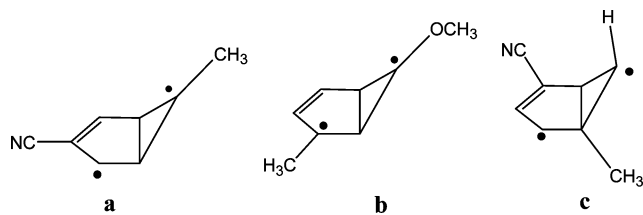


Figure 6. The CASPT2 relative energies (kcal mol^{-1}) of isomerization from p-methylanisole to m-methylanisole and o-methylanisole.

SCHEME 6



SCHEME 7



sponding S_1/S_0 conical intersection on the S_1 PES. Furthermore, no stable prefulvene biradicals can be formed owing to lack of conjugated interactions stabilizing the unpaired electron. However, the presence of $-\text{OCH}_3$ group may stabilize the carbene structure. Once the S_1/S_0 conical intersection is accessible, the photoisomerization of p-, m-, and o-methylanisoles is also plausible through the carbene mechanism, although its isomerization efficiency should be lower than that of methylbenzotrienes.

Present calculations suggest that the accessibility of S_1/S_0 conical intersection should be the crucial factor to dominate photoisomerization activity for p-, m-, and o-substituted ben-

zenes at 254 nm. The results provide some insight into the photochemistry of substituted benzenes.

Acknowledgment. This work was supported by the National Science Foundation of China (Grants 20673087, 20473062, 20423002, 20233020) and the Ministry of Science and Technology (Grant 2004CB719902).

Supporting Information Available: Detailed discussion of the 1,2-H shift mechanism, including optimized structures and relative energy diagrams, and the B3LYP-optimized ground state structures of **A1**, **A2/A3**, and **A4**. This material is available free of charge via the Internet at <http://pubs.acs.org>.

References and Notes

- (1) Wilzbach, K. E.; Kaplan, L. *J. Am. Chem. Soc.* **1964**, *86*, 2307–2308.
- (2) Kaplan, L.; Wilzbach, K. E.; Brown, W. G.; Yang, S. S. *J. Am. Chem. Soc.* **1965**, *87*, 675–676.
- (3) Burgstahler, A. W.; Chien, P. L. *J. Am. Chem. Soc.* **1964**, *86*, 2940, and references therein.
- (4) (a) Palmer, I. J.; Ragazos, I. N.; Bernardi, F.; et al. *J. Am. Chem. Soc.* **1993**, *115*, 673–682, and references therein. (b) Robb, M. A.; Garavelli, M.; Olivucci, M.; Bernardi, F. *Rev. Comp. Chem.* **2000**, *15*, 87, and references therein. (c) Sobolewski, A. L. *J. Chem. Phys.* **1990**, *93*, 6433–6439.
- (5) Turro, N. J.; Renner, C. A.; Katz, T. J.; Wiberg, K. B.; Cannon, H. A. *Tetrahedron Lett.* **1976**, 4133.
- (6) MacLeod, P. J.; Pincock, A. L.; Pincock, J. A.; Thompson, K. A. *J. Am. Chem. Soc.* **1998**, *120*, 6443–6450.
- (7) Foster, J.; Pincock, A. L.; Pincock, J. A.; Thompson, K. A. *J. Am. Chem. Soc.* **1998**, *120*, 13354–13361.
- (8) (a) Foster, J.; Pincock, A. L.; Pincock, J. A.; Rifai, S.; Thompson, K. A. *Can. J. Chem.* **2000**, *78*, 1019–1029. (b) González, C. M.; Pincock, J. A. *J. Am. Chem. Soc.* **2004**, *126*, 8870–8871.
- (9) Becke, A. D. *J. Chem. Phys.* **1993**, *98*, 5648.
- (10) Lee, C.; Yang, W.; Parr, R. G. *Phys. Rev.* **1988**, *B37*, 785.
- (11) Frisch, M. J.; Trucks, G. W.; Schlegel, H. B.; Scuseria, G. E.; Robb, M. A.; Cheeseman, J. R.; Zakrzewski, V. G.; Montgomery, J. A. Jr.; Stratmann, R. E.; Burant, J. C.; Dapprich, S.; Millam, J. M.; Daniels, A. D.; Kudin, K. N.; Strain, M. C.; Farkas, O.; Tomasi, J.; Barone, V.; Cossi, M.; Cammi, R.; Mennucci, B.; Pomelli, C.; Adamo, C.; Clifford, S.; Ochterski, J.; Petersson, G. A.; Ayala, P. Y.; Cui, Q.; Morokuma, K.; Malick,

- D. K.; Rabuck, A. D.; Raghavachari, K.; Foresman, J. B.; Cioslowski, J.; Ortiz, J. V.; Stefanov, B. B.; Liu, G.; Liashenko, A.; Piskorz, P.; Komaromi, I.; Gomperts, R.; Martin, R. L.; Fox, D. J.; Keith, T.; Al-Laham, M. A.; Peng, C. Y.; Nanavakkara, A.; Gonzalez, C.; Challacombe, M.; Gill, P. M. W.; Johnson, B.; Chen, W.; Wong, M. W.; Andres, J. L.; Gonzalez, C.; Head-Gordon, M.; Replogle, E. S.; Pople, J. A. *Gaussian 03*, Revision B.03; Gaussian, Inc.; Pittsburgh, PA, 2003.
- (12) (a) Werner, H.-J.; Knowles, P. J. *J. Chem. Phys.* **1985**, *82*, 5053. (b) Knowles, P. J.; Werner, H.-J. *Chem. Phys. Lett.* **1985**, *115*, 259. (c) Busch, T.; Degli Esposti, A.; Werner, H.-J. *J. Chem. Phys.* **1991**, *94*, 6708. (d) Roos, B. O. In *Ab Initio Methods in Quantum Chemistry II*; Lawley, K. P., Ed.; Wiley: New York, 1987; p 399.
- (13) (a) Werner, H.-J. *Mol. Phys.* **1996**, *89*, 645. (b) Celani, P.; Werner, H.-J. *J. Chem. Phys.* **2000**, *112*, 5546.
- (14) Casida, M. E.; Jamorski, C.; Casida, K. C.; Salahub, D. R. *J. Chem. Phys.* **1998**, *108*, 4439.
- (15) Hampel, C.; Peterson, K.; Werner, H.-J. *Chem. Phys. Lett.* **1992**, *190*, 1.
- (16) MOLPRO, version 2002.1, a package of ab initio programs designed by Werner, H.-J.; Knowles, P. J.; Amos, R. D.; Bernhardsson, A.; Berning, A.; Celani, P.; Cooper, D. L.; Deegan, M. J. O.; Dobbyn, A. J.; Eckert, F.; Hampel, C.; Hetzer, G.; Knowles, P. J.; Korona, T.; Lindh, R.; Lloyd, A. W.; McNicholas, S. J.; Manby, F. R.; Meyer, W.; Mura, M. E.; Nicklass, A.; Palmieri, P.; Pitzer, R.; Rauhut, G.; Schütz, M.; Schumann, U.; Stoll, H.; Stone, A. J.; Tarroni, R.; Thorsteinsson, T.; Werner, H.-J.
- (17) (a) Herhe, W. J.; Ditchfield, R.; Pople, J. A. *J. Chem. Phys.* **1972**, *56*, 2257. (b) Harihan, P. C.; Pople, J. A. *Theor. Chim. Acta.* **1973**, *28*, 213.
- (18) Ishida, T.; Hirata, F.; Kato, S. *J. Chem. Phys.* **1999**, *110*, 11432.
- (19) Dreuw, A.; Head-Gordon, M. *Chem. Rev.* **2005**, *105*, 4009–4037.
- (20) Bettinger, H. F.; Schreiner, P. R.; Schaefer, III, H. F.; Schleyer, P. R. *J. Am. Chem. Soc.* **1998**, *120*, 5741–5750.
- (21) (a) Sobolewski, A. L.; Domke, W. *Chem. Phys. Lett.* **1991**, *180*, 381–386. (b) Sobolewski, A. L.; Woywod, C.; Domcke, W. *J. Chem. Phys.* **1993**, *98*, 5627–5641.
- (22) Kato, S. *J. Chem. Phys.* **1988**, *88*, 3045–3056.
- (23) Dreyer, J.; Klessinger, M. *Chem. Eur. J.* **1996**, *2*, 335.
- (24) Merz, K. M.; Scott, L. T. *Chem. Commun.* **1993**, 412.
- (25) Alvarez-Valtierra, L.; Yi, J. T.; Pratt, D. W. *J. Phys. Chem. B* **2006**, *110*, 19914–19922.
- (26) Zimmerman, H. E.; Mitkin, O. D. *J. Am. Chem. Soc.* **2006**, *128*, 12743–12749.